Article title: Nanocomposite Coated Carbon-MEMS-Derived Glassy Carbon Electrode for Acetone Sensing.

Journal name: SPRINGER- Microsystem Technologies (Extended version of Micro/Nanoelectronics Devices, Circuits and Systems (MNDCS-2026).

Anto Manuel[1,2] [0009-0009-2438-4567],
Madhukumar S[2] [0000-0002-2422-5891], and
Bidhan Pramanick[1,3*] [0000-0001-9792-2383]

[1]School of Electrical Sciences, Indian Institute of Technology (IIT) Goa, Farmagudi, Ponda, 403401, Goa, India.
[2]Department of Biomedical Engineering, Rajadhani Institute of Engineering and Technology, Trivandrum, 695102, Kerala, India.
[3]Center of Excellence in Particulates, Colloids and Interfaces, Indian Institute of Technology (IIT) Goa, Farmagudi, Ponda, 403401, Goa, India.
bidhan@iitgoa.ac.in, anto20242201@iitgoa.ac.in.

Supplementary Materials (SM)

1 Supplementary part of Section 3.1 Materials

SM Table 1: Details of Materials and Sources

Sl. No.	Material	Obtained from
1	Silicon Wafer (⟨100⟩, p-type, 2-inch)	Siltronic, Germany
2	SiO_2 Layer	Thermal oxidation (Dry–Wet–Dry: 20–120–20 min at 1000°C)
3	SU-8 2010 (Negative PR)	MicroChem Corp., USA
4	Silver Conductive Paste (Code 842)	M.G. Chemicals, Canada
5	Ethylene Glycol (CAS: 107-21-1)	Avra Synthesis Pvt. Ltd., India
6	TiO_2 Nanopowder ($\geq$99.5%)	Sigma-Aldrich, China
7	ZnO (99.999% purity)	Sigma-Aldrich, China
8	Acetone (C_3H_6O)	SimSon PharmaChem, Mumbai, India
9	Carbon Nanotubes (CNTs)	Sigma-Aldrich, USA

2 Supplementary part of Section 3.3 Fabrication of GC–IDE

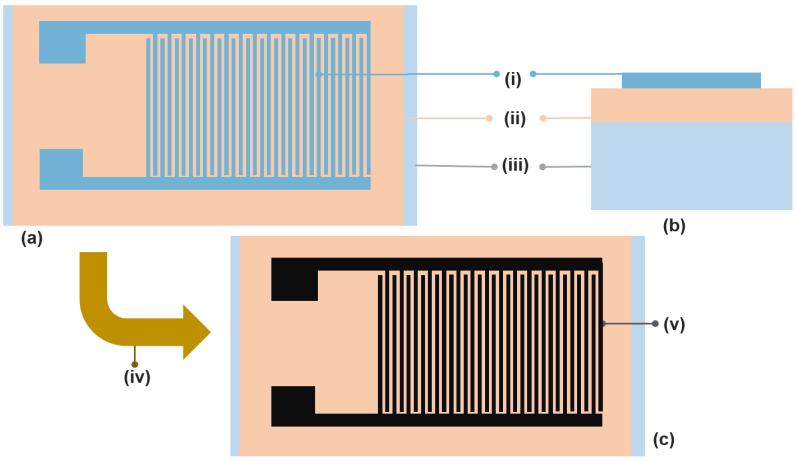

SMFig. 1: The SU-8 PR structure transition to a GC–IDE is shown graphically in (a) the SU8 PR structure created by the photolithography process following the spin coat of PR, (b) a cross-sectional view of (a), and (c) the GC–IDE structure developed following the pyrolysis process that converted the SU-8 PR structure to GC–IDE ((i): SU8 PR Structure, (ii): SiO_2 layer, (iii): Si Substrate, (iv): Pyrolysis Process at 1000°C, (v): GC–IDE).

Fig. 1 illustrates the transition of an SU-8 PR structure into a GC–IDE through the pyrolysis process. The comprehensive process described in Ref [**?**] was followed in order to convert SU-8 PR into GC–IDE.

A 2-inch ⟨100⟩ p-type silicon wafer was used as the substrate for IDE fabrication.

During this high-temperature treatment, the SU-8 PR polymer undergoes thermal decomposition and carbonization, resulting in the formation of a GC–IDE, as shown in Fig. 1(c).

3 Supplementary part of Section 4.3 Interaction of Nanocomposite with Acetone

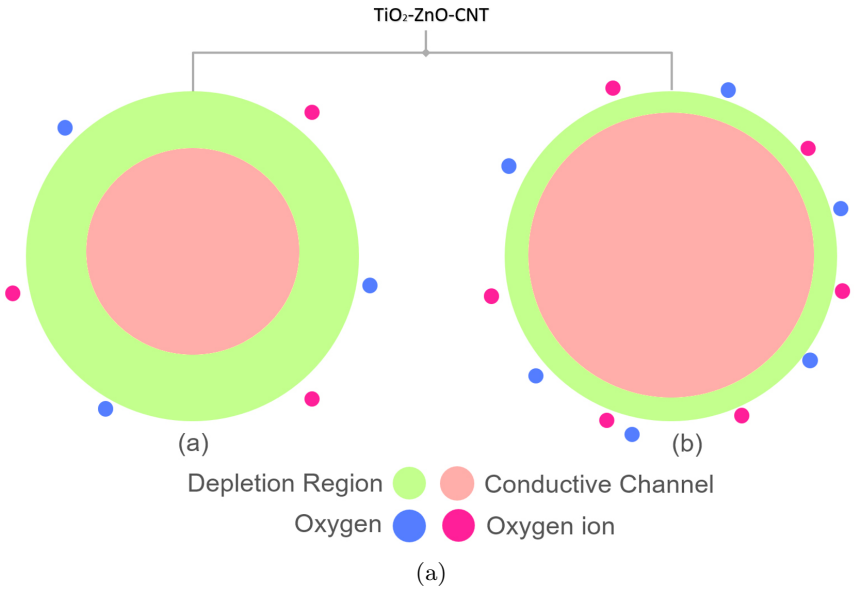

(a)

SMFig. 2: Schematics of the electrical structures of the TiO_2–ZnO–CNT (a) In the presence of ((a)Air, (b)Acetone).

SM Table 2: Results obtained using Parametric Analyzer: Voltage, current and resistance change in the exposure and absence of acetone (SL1 and SL2) *(Supplementary part of Section 4.4 Results Obtained with the aid of Parametric Analyzer, Fig. 8a, 8b, 9a, 9b, 10a and 10b (CAA: Current in the absence of Acetone, RAA: Resistance in the absence of Acetone, CPA: Current in the presence of Acetone, RPA: Resistance in the presence of Acetone).*

	Figure 7a		Figure 7b		Figure 8a and 8b		Figure 8c and 8d	
Voltage (V)	CAA (A)	RAA (Ω)	CPA (A)	RPA (Ω) (A)	Time (s)	RPA (Ω) (A)	Time (s)	RPA (Ω)
1.0	1.0E-9	1.05E9	4.3E-7	2.31E6	1	1.81E6	1	1.33E6
1.1	1.4E-9	8.10E8	5.2E-7	2.11E6	7	2.06E6	8	8.58E5
1.2	1.2E-9	1.04E9	6.0E-7	2.00E6	13	2.28E6	15	8.69E5
1.3	1.3E-9	9.50E8	6.8E-7	1.91E6	19	2.33E6	23	7.72E7
1.4	1.4E-9	9.85E8	7.6E-7	1.84E6	25	2.69E6	30	2.15E8
1.5	2.1E-9	7.20E8	8.2E-7	1.83E6	31	1.01E7	37	3.76E8
1.6	1.6E-9	9.70E8	9.1E-7	1.76E6	37	3.21E7	47	4.96E8
1.7	2.7E-9	6.30E8	9.9E-7	1.70E6	44	7.87E7	60	5.05E8
1.8	1.8E-9	9.55E8	1.10E-6	1.64E6	51	9.97E7	72	5.19E8
1.9	2.6E-9	7.30E8	1.18E-6	1.61E6	57	2.16E8	85	5.26E8
2.0	2.0E-9	9.90E8	1.28E-6	1.56E6	63	2.66E8	98	5.30E8
2.1	2.9E-9	7.40E8	1.42E-6	1.48E6	69	3.78E8	106	5.31E8
2.2	2.2E-9	9.80E8	1.56E-6	1.41E6	75	3.97E8	115	5.33E8
2.3	3.4E-9	6.60E8	1.67E-6	1.38E6	81	4.98E8	131	5.34E8
2.4	2.5E-9	9.20E8	1.78E-6	1.35E6	88	5.11E8	144	5.38E8
2.5	4.0E-9	6.25E8	1.90E-6	1.32E6	93	5.21E8	—	—
2.6	4.1E-9	6.50E8	2.04E-6	1.28E6	98	5.41E8	—	—
2.7	4.2E-9	6.40E8	2.18E-6	1.24E6	105	5.50E8	—	—
2.8	4.4E-9	6.40E8	2.32E-6	1.21E6	112	5.77E8	—	—
2.9	4.6E-9	6.30E8	2.44E-6	1.19E6	119	6.07E8	—	—
3.0	4.8E-9	6.25E8	2.58E-6	1.16E6	128	6.31E8	—	—
3.1	5.0E-9	6.20E8	2.73E-6	1.14E6	136	6.42E8	—	—
3.2	5.2E-9	6.15E8	2.88E-6	1.11E6	144	6.51E8	—	—
3.3	5.3E-9	6.25E8	3.02E-6	1.09E6	153	6.61E8	—	—
3.4	5.6E-9	6.10E8	3.18E-6	1.07E6	161	6.77E8	—	—
3.5	5.8E-9	6.05E8	3.33E-6	1.05E6	174	6.98E8	—	—
3.6	6.1E-9	5.90E8	3.45E-6	1.04E6	182	7.08E8	—	—
3.7	6.2E-9	5.95E8	3.62E-6	1.02E6	191	7.25E8	—	—
3.8	6.4E-9	5.90E8	3.76E-6	1.01E6	200	7.42E8	—	—
3.9	6.6E-9	5.85E8	3.93E-6	9.90E5	212	7.60E8	—	—
4.0	6.9E-9	5.80E8	4.10E-6	9.80E5	218	7.69E8	—	—
4.1	7.2E-9	5.70E8	4.26E-6	9.60E5	228	7.69E8	—	—
4.2	7.5E-9	5.60E8	4.42E-6	9.50E5	—	—	—	—
4.3	7.7E-9	5.65E8	4.57E-6	9.40E5	—	—	—	—
4.4	7.8E-9	5.60E8	4.76E-6	9.20E5	—	—	—	—
4.5	8.1E-9	5.55E8	4.94E-6	9.10E5	—	—	—	—
4.6	8.3E-9	5.55E8	5.08E-6	9.00E5	—	—	—	—
4.7	8.5E-9	5.50E8	5.26E-6	8.90E5	—	—	—	—
4.8	8.7E-9	5.50E8	5.42E-6	8.80E5	—	—	—	—
4.9	8.9E-9	5.45E8	5.59E-6	8.70E5	—	—	—	—
5.0	9.3E-9	5.38E8	5.83E-6	8.60E5	—	—	—	—